Overactive WASp in X-linked neutropenia leads to aberrant B-cell division and accelerated plasma cell generation

Minghui He, PhD,[a] Mezida B. Saeed, PhD,[a] Julien Record, PhD,[a] Marton Keszei, PhD,[a] Lia Gonçalves Pinho, MSc,[a,b] Larissa Vasconcelos-Fontes, PhD,[a,b] Roberta D'Aulerio, MSc,[a] Rhaissa Vieira, PhD,[a] Mariana M. S. Oliveira, MSc,[a] Chiara Geyer, MSc,[a] Lena Bohaumilitzky, MSc,[a] Meike Thiemann, MSc,[a] Ekaterina Deordieva, PhD,[c] Lieselot Buedts, PhD,[d] Joao Pedro Matias Lopes, MSc,[e,f] Dmitry Pershin, PhD,[c] Lennart Hammarström, MD, PhD,[g] Yu Xia, MD,[h] Xiaodong Zhao, MD, PhD,[i] Charlotte Cunningham-Rundles, MD, PhD,[e] Adrian J. Thrasher, MD, PhD,[j,k] Siobhan O. Burns, MD, PhD,[l,m] Vinicius Cotta-de-Almeida, PhD,[b] Chaohong Liu, PhD,[n] Anna Shcherbina, MD, PhD,[c] Peter Vandenberghe, MD, PhD,[d] and Lisa S. Westerberg, PhD[l] *Stockholm, Sweden; Rio de Janeiro, Brazil; Moscow, Russia; Leuven, Belgium; New York, NY; Cleveland, Ohio; Shenzhen, Chongqing, and Wuhan, China; and London, United Kingdom*

GRAPHICAL ABSTRACT

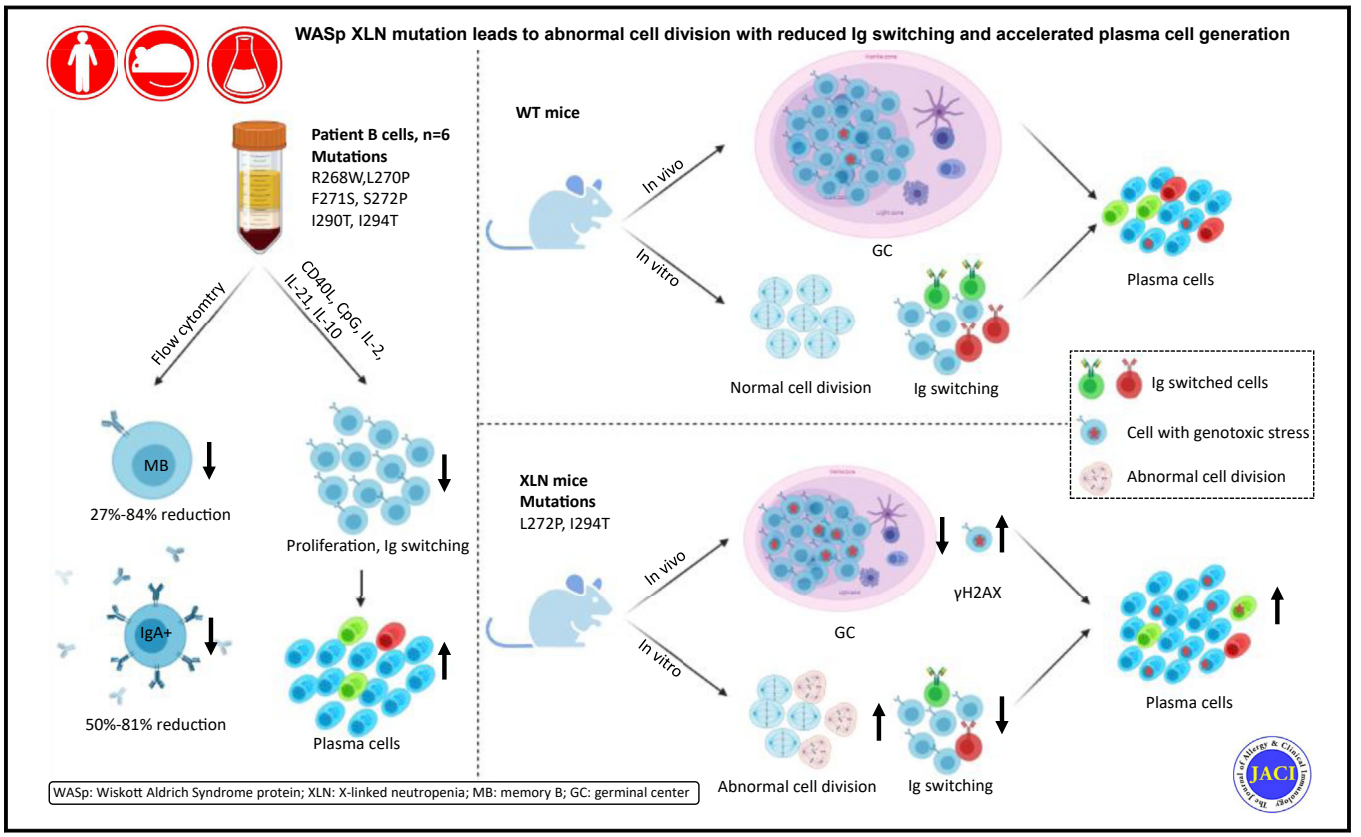

From [a]the Department of Microbiology Tumor and Cell Biology, Karolinska Institutet, Stockholm; [b]the Laboratory on Thymus Research, Oswaldo Cruz Institute, Fiocruz, Rio de Janeiro; [c]the Department of Immunology, Dmitry Rogachev National Medical and Research Center of Pediatric Hematology, Oncology and Immunology, Moscow; [d]the Center for Human Genetics, University Hospital Leuven, Leuven; [e]the Department of Pediatrics, Icahn School of Medicine at Mount Sinai, New York; [f]the Division of Allergy, Immunology and Rheumatology, Department of Pediatrics, UH Rainbow Babies and Children's Hospital, Cleveland; [g]the Department of Laboratory Medicine, Karolinska Institutet, Stockholm; [h]the Department of Rheumatology and Immunology, Shenzhen Children's Hospital, Shenzhen; [i]the Chongqing Key Laboratory of Child Infection and Immunity, Children's Hospital of Chongqing Medical University, Chongqing; [j]the UCL Great Ormond Street Institute of Child Health, London; [k]the Great Ormond Street Hospital for Children NHS Foundation Trust, London; [l]the Department of Immunology, Royal Free London NHS Foundation Trust, London; [m]the Institute of Immunity and Transplantation, University College London, London; and [n]the Department of Pathogen Biology, School of Basic Medicine, Huazhong University of Science and Technology, Wuhan.

Supported by a postdoctoral fellowship from Olle Engqvist Byggmästare to M.H., a postdoctoral fellowship from Wenner-Gren foundations to M.S., postdoctoral fellowships from the Childhood Cancer Fund and the Swedish Society for Medical Research to J.R., a postdoctoral fellowship from the Cancer Society to M.K., a CAPES-STINT joint grant to V.C.d.A. and L.S.W., the Swedish Research Council, Cancer Society, Childhood Cancer Fund, a StratCan BlueSky award, the European Commission 7th framework program Marie Curie reintegration grant (grant 249177), the Åke Olsson Foundation, the Åke Wiberg Foundation, the Bergvall Foundation, King Gustaf V's 80-Year Foundation, and Karolinska Institutet to L.S.W. L.S.W. is a Ragnar Söderberg fellow in Medicine and holds a senior researcher position supported by the Childhood Cancer Fund.

Disclosure of potential conflict of interest: The authors declare that they have no relevant conflicts of interest.

Background: B-cell affinity maturation in germinal center relies on regulated actin dynamics for cell migration and cell-to-cell communication. Activating mutations in the cytoskeletal regulator Wiskott-Aldrich syndrome protein (WASp) cause X-linked neutropenia (XLN) with reduced serum level of IgA.
Objective: We investigated the role of B cells in XLN pathogenesis.
Methods: We examined B cells from 6 XLN patients, 2 of whom had novel R268W and S271F mutations in WASp. By using immunized XLN mouse models that carry the corresponding patient mutations, WASp L272P or WASp I296T, we examined the B-cell response.
Results: XLN patients had normal naive B cells and plasmablasts, but reduced IgA^+ B cells and memory B cells, and poor B-cell proliferation. On immunization, XLN mice had a 2-fold reduction in germinal center B cells in spleen, but with increased generation of plasmablasts and plasma cells. *In vitro,* XLN B cells showed reduced immunoglobulin class switching and aberrant cell division as well as increased production of immunoglobulin-switched plasma cells.
Conclusions: Overactive WASp predisposes B cells for premature differentiation into plasma cells at the expense of cell proliferation and immunoglobulin class switching. (J Allergy Clin Immunol 2021;■■■:■■■-■■■.)

Key words: *B cells, X-linked neutropenia, actin, WASp, IgA, germinal center, plasma cells, primary immunodeficiency*

Abbreviations used

BCR:	Breakpoint cluster region
BSA:	Bovine serum albumin
CSR:	Class switch recombination
DZ:	Dark zone
GBD:	GTPase binding domain
GC:	Germinal center
iGB:	Inducible GC B-cell culture system
KLH:	Keyhole limpet hemocyanin
LPS:	Lipopolysaccharide
LZ:	Light zone
MHC:	Major histocompatibility complex
MZ:	Marginal zone
NP:	4-Hydroxy-3-iodo-5-nitrophenylacetyl
N-WASp:	Neuronal WASp
PBMC:	Peripheral blood mononuclear cell
SRBC:	Sheep red blood cell
WAS:	Wiskott-Aldrich syndrome
WASp:	WAS protein
WT:	Wild type
XLN:	X-linked neutropenia

B-cell affinity maturation takes place in germinal center (GC) and is an important feature of all vaccination approaches to obtain production of high-affinity antibodies. The GC is divided into a dark zone (DZ) and a light zone (LZ). In the DZ, B cells upregulate activation-induced cytidine deaminase that induces somatic hypermutation of the immunoglobulin variable genes and immunoglobulin class switch recombination (CSR) from IgM to IgG, IgA, and IgE subtypes.[1] The newly mutated and immunoglobulin class switched B cells migrate from the DZ to LZ to test their breakpoint cluster region (BCR) for antigen recognition on antigen-covered follicular dendritic cells.[2-6] B cells extract antigens deposited on follicular dendritic cells through pulling forces that are mediated by actin and myosin contraction.[7,8] The high-affinity B cells will leave the GC as memory B cells and plasma cells.[9] Plasma cell differentiation is coupled to cell proliferation with upregulation of *IRF4* after 4 cell divisions.[10-12]

Actin cytoskeleton is important during the B-cell immune response, as is evident in actin-related primary immunodeficiency diseases such as Wiskott-Aldrich syndrome (WAS).[13-15] B cells of WAS patients and WAS protein (WASp)-deficient animals have reduced capacity to mount an antibody response to non–self-antigen challenge[16-18] but produce autoantibodies of both IgM and IgG isotypes.[19-23] Deletion of both WASp and the homologous protein neuronal (N)-WASp in B cells ameliorate autoantibody production,[20,21] and a complex signaling competition between WASp and N-WASp occurs during early BCR signaling.[24-26] Defective B-cell responses are restored to normal in patients that have undergone gene therapy to correct WAS gene expression.[27,28]

WASp activity is regulated by structural conformation and WASp resides as an inactive form in the cytoplasm.[13] The interaction of the WASp GTPase binding domain (GBD) with GTP-bound Cdc42 releases the autoinhibition and exposes the carboxy terminal verprolin cofilin acidic domain for actin polymerization.[13,29,30] Point mutations in the WASp GBD domain lead to X-linked neutropenia (XLN), a severe form of congenital neutropenia with clinical manifestation vastly different from WAS.[31-33] Whereas WAS is caused by reduced or abolished expression of WASp,[34] XLN mutations of WASp destroy the intramolecular autoinhibition and render WASp constitutively active.[31-33,35,36] To date, 4 XLN mutations in WASp have been described: WAS L270P, I294T, S272P, and I290T.[31-33,37,38] Our initial study of WAS L270P patients and XLN mouse models showed that XLN neutrophils are hyperactive in regards to migration into tissues and effector function.[36]

To understand B-cell differentiation and functional responses, we analyzed 6 XLN patients with *WAS* mutations, including 2 with de novo R268W and S271F mutations predicted to be pathogenic. We found that XLN patient B cells had low IgA switching, reduced memory cells, and decreased cell proliferation. Despite defective GC response and impaired cell proliferation, XLN B cells had increased formation of plasma cells both *in vivo* and *in vitro*. Our data show that overactive WASp in XLN leads to accelerated plasma cell generation at the expense of GC formation and immunoglobulin class switching, especially to IgA.

Received for publication April 29, 2021; revised July 19, 2021; accepted for publication July 23, 2021.

Corresponding authors: Minghui He, PhD, Karolinska Institutet, Department of Microbiology, Tumor and Cell Biology, Biomedicum C7, Stockholm, Sweden. E-mail: Minghui.He@ki.se. Or: Lisa S. Westerberg, PhD, Karolinska Institutet, Department of Microbiology, Tumor and Cell Biology, Biomedicum C7, Stockholm, Sweden. E-mail: Lisa.Westerberg@ki.se.

0091-6749

https://doi.org/10.1016/j.jaci.2021.07.033

METHODS

Patients

Peripheral blood samples were analyzed from 6 XLN patients, their healthy relatives, and unrelated healthy controls that were sex and age matched to the XLN patients. Peripheral blood mononuclear cells (PBMCs) were isolated and stained for flow cytometry analysis. The Code of Ethics of the World Medical Association (Declaration of Helsinki) for human samples was followed, the study was approved by the institutional review boards, and written consent was obtained from all individuals.

Mice and cell transfers

The WASp L272P and WASp I296T mice were generated as previously described[36] and housed under specific-pathogen-free conditions at the animal facility of Comparative Medicine, Karolinska Insitutet. All animal experiments performed were approved by the Stockholm North animal ethics committee (permits N272/14 and 11159-18). To generate mixed bone marrow chimeric mice, CD45.1 WT cells and CD45.2 XLN or WASp$^{-/-}$ cells were injected intravenously to the lethally irradiated CD45.1/CD45.2 heterozygous congenic mice.

B-cell isolation and iGB cell culture

Mouse splenic B cells were enriched by the negative B-cell selection Kit from Stem Cell Technology. B cells were cultured on irradiated 40LB cells as previously.[39] Cell culture was supplemented with IL-4 and on day 4, with IL-21 and analyzed on day 7 or 8 by flow cytometry.

Immunization, flow cytometry, ELISA, and tissue sections

Mice were immunized with sheep red blood cells (SRBCs) via intraperitoneal injection. On day 7, single-cell suspensions were prepared and labeled with fluorescence-conjugated antibodies for flow cytometry. For antigen-specific response, mice were immunized intraperitoneally with 4-hydroxy-3-iodo-5-nitrophenylacetyl (NP) keyhole limpet hemocyanin (KLH; Biosearch Technologies, Hoddesdon, United Kingdom) in Imject Alum Adjuvant (Thermo Fisher Scientific, Waltham, Mass), followed by a second injection NP-KLH at day 21. On day 28, cells were prepared for flow cytometry. Data were obtained by LSRFortessa flow cytometry (Becton Dickinson, San Diego, Calif) and analyzed with FlowJo software (Treestar, Ashland, Ore). For ELISA, serum was collected from NP-KLH immunized mice on day 0, day 21, and day 28. Serum IgG against NP8–bovine serum albumin (BSA) or NP25-BSA was detected as previously described.[20] Spleen sections were fixed in ice-cold acetone and incubated with primary and secondary antibodies.

Cell signaling and receptor internalization

Lipopolysaccharide (LPS)-activated B cells were treated with TGF-β at the indicated time points and fixed. A standard phosphoFlow protocol (Becton Dickinson, San Diego, Calif) was performed to detect phosphor-Smad2/Smad3. To inhibit the Smad2/3 phosphorylation, SB431542 (Sigma-Aldrich, St Louis, Mo) was added. To detect receptor internalization, LPS-activated B cells were stained with biotinylated anti-IgM or anti–TGF-β receptor II for the time points indicated and fixed for flow cytometry analysis.

Western blot analysis

Naive B cells or LPS-activated B cells were collected, and protein extracts were prepared as previously described to detect WASp.[36] WASp was immunoprecipitated with an anti-WASp antibody (F8), and the immunoblot was developed with anti-WASp (F8; Santa Cruz Biotechnology, Santa Cruz, Calif) or anti-WASp phospho-Y293 antibody (Abcam, Cambridge, United Kingdom).

Time-lapse imaging of cell division and B-cell spreading

B cells from the inducible GC B-cell (iGB) cell culture system at day 4 were placed in a microscope environmental chamber at 37°C. Cell division was imaged every 2 minutes at 37°C with 5% CO_2 using a Zeiss (Jena, Germany) CellObserver Z1 device equipped with an EC Plan-Neofluar 10×/0.30 Ph1 objective and a Zeiss Axiocan MR R3 camera. For B-cell spreading assays, splenic B cells were added to anti–IgM- and anti–IgG-coated coverslips, fixed, and labeled with phalloidin. Cells were imaged on a Zeiss LSM800-Airy microscope, and high-resolution images were obtained using 3D Airyscan processing in ZEN Lite software (Zeiss). Images were processed and analyzed using ImageJ (https://imagej.nih.gov/ij/) or Fiji (https://fiji.sc/) software.

Statistical analysis

Statistical analysis was performed using the Prism software (versions 6-8, GraphPad) by unpaired *t* test, 1-way ANOVA, or 2-way ANOVA as indicated.

RESULTS

XLN patients have decreased IgA$^+$ B cells in circulation, and decreased B-cell proliferation and increased differentiation of plasma cells *in vitro*

We collected patient cells from 2 brothers with the WAS L270P mutation[32,36] and from 4 new patients, 1 of whom had a WAS I294T mutation described previously in other XLN patients,[31,33] 1 of whom had a novel WAS F271S mutation, 1 of whom had a novel WAS R268W mutation, and 1 of whom had a WAS I290T mutation.[38] Clinical analysis of these 6 patients plus the 3 additional patients previously described revealed that all patients had congenital neutropenia (Table I, I294T UK, S272P UK, I294T Ireland).[40] Structural prediction shows that the new mutations WAS F271S and R268W are proximal to the described L270P and S272P mutations in the alpha helix of the WASp GBD, and the I294T and I290T mutations are localized in the adjacent alpha helix in the 3D structure of the WASp GBD (Fig 1, *A*). All XLN mutations identified to date are replacing highly conserved amino acids in the WAS GBD and are predicted to be disruptive using PolyPhen and SIFT (sorting intolerant from tolerant) prediction (Fig 1, *A*). The frequency of different cell subsets was analyzed by flow cytometry of isolated PBMCs. There were similar proportion of CD3$^+$ T cells and CD20$^+$ B cells in healthy donors and XLN patients (see Fig E1, *A-H,* in this article's Online Repository at www.jacionline.org). Compared to the controls, 5 XLN patients had decreased CD38$^-$CD24$^+$ memory B cells, and no firm conclusion could be drawn of P11 as a result of a lack of a pediatric control (Fig 1, *B* and *C,* and see Fig E2 in this article's Online Repository at www.jacionline.org). All tested patients showed low serum IgA, except 2 pediatric patients (P11 and P12) who had normal serum IgA (Table I). All patients tested had reduced IgA$^+$IgD$^-$ switched B cells (Fig 1, *B* and *C,* and Fig E2). WAS L270P, F271S, and I294T patients had reduced IgA$^+$CD27$^+$ memory cells, whereas R268W and I290T patients had too few cells to measure (Fig E1, *A-H*). All patients (except for the WAS I290T patient whose PBMCs were poorly recovered from blood) had increased CD38$^+$CD24$^+$ transitional B cells (Fig 1, *B* and *C,* and Fig E2). CD38$^+$CD24$^-$ plasmablasts were detected in all samples, albeit at low frequency (Fig 1, *B* and *C,* and Fig E2).

To understand how XLN B cells generated immunoglobulin switched and nonswitched plasma cells *in vitro,* we sorted CD20$^+$CD27$^-$ naive B cells from the WAS F271S and WAS

TABLE I. Hematologic and immunologic parameters XLN patients

Characteristic	Patient no. P1	P2	P12	P4	P5	P8	P11	P	P	Adult range	Pediatric range
Country	Belgium	Belgium	China	UK	Russia	Russia	USA	UK	Ireland*	—	—
WASp	L270P	L270P	I290T	I294T	F271S	I294T	R268W	S272P	I294T	—	—
WAS gene	T809C†	T809C†	T869C	T881C	T812C	T881C	C802T	T814C	T881C	—	—
Mother carrier status	L270P/+	L270P/+	ND	I294T/+	ND	I294T/+	R268W/+	ND	I294T/+	—	—
Year of sampling: age (years)	2016: 26	2016: 21	2018: 4	2018: 19	2019: 16	2019: 5	2020: 1	NA	NA	—	—
GCSF	No	No	No	No	5 μg/kg/d 1 in 3 days	15 μg/kg/d	No	3 μg/kg	—	—	—
Neutrophils Blood ($\times 10^9$/L)	0.1	0.2	0.2-0.5	0.17-0.47	0.28	0.32	0.1-0.5	0.05-0.26	0.1-2.4	2.0-7.8	2.2—5.7
Neutrophils in saliva	Yes	Yes	Yes	Yes	ND	ND	ND	ND	ND	Yes	Yes
B lymphocytes ($\times 10^9$/L)	0.07-0.18‡	0.07-0.18‡	1.29	ND	0.26	1.08	ND	ND	0.075-0.42	0.20-0.50	0.5-1.5
IgM (g/L)	0.22	0.80	0.62	ND	1.24	0.647	1.24	ND	ND	0.8-1.9	0.6-1.8
IgG (g/L)	8.84	13.8	4.18	ND	10.5	7.52	9.04	ND	ND	8.7-11.7	4.6-14.6
IgA (g/L)	0.17	0.48	0.52	ND	0.535	0.03	0.68	ND	0.29-1.49	0.80-2.80	0.1-1
IgE (g/L)	ND	ND	ND	ND	102	2.14	ND	ND	ND	0-100	0-100
Leucocytes ($\times 10^9$/L)	2.05	2.86	2.5-2.9	0.9-3.29	2.34	4.64	4.3-12.4	2.7-5.6	1.7-5.2	4.0-11	6.0-9.9
Monocytes ($\times 10^9$/L)	0.0	0.0	0.35-0.86	0.05-0.22	0	0.139	0.2-1.0	ND	0.1-0.4	0.2-1.5	0.24-0.89
Eosinophils ($\times 10^9$/L)	0.1	0.1	0.01-0.12	ND	0.28	0.185	0-0.3	ND	0-0.2	0.02-0.5	0.061-0.69
Platelets ($\times 10^9$/L)	195	182	88-206	153-218	186	203	150-450	172-353	96-279	150-450	204-356
Lymphocytes ($\times 10^9$/L)	1.8	1.5	1.4-2.1	0.48-2.59	1.73	3.75	1.6-5.9	0.84-5.83	0.7-2.6	1.0-3.0	1.9-5.2
T lymphocytes $CD3^+$ ($\times 10^9$/L)	1.75-3.65‡	1.75-3.65‡	1.05	ND	1.51	2.89	1.898	ND	0.69-2.29	0.8-2.0	1.4-5.4
$CD4^+$ T cells ($\times 10^9$/L)	0.55-1.14‡	0.55-1.14‡	0.31	0.23-0.53	0.76	1.59	1.48	1.1	0.20-1.34	0.5-1.1	1.0-3.6
$CD8^+$ T cells ($\times 10^9$/L)	1.20-2.58‡	1.20-2.58‡	0.71	0.24-0.45	0.58	1.16	0.39	0.87	0.34-0.94	0.5-0.9	0.5-2.2
CD4/CD8 ratio	0.42-0.5‡	0.42-0.5‡	0.450	0.93	1.31	1.363	3.76	1.26	0.4-1.53	1.1-3.2	1-3
NK cells ($\times 10^9$/L)	0.01-0.11‡	0.01-0.11‡	0.07	0.01-0.03	0.03	0.008	.018	0.02	0.02-0.04	0.20-0.8	0.27-0.89
BM Lymphocytes (%)	ND	ND	32	ND	32	61.6	ND	ND	ND	4.3-13.7	10.2-16.4
BM granulocytes (%)	Low	Low	55.5	Low	14	12	ND	ND	ND	52.7-68.9	36.4-68
BM blast cells (%)	ND	ND	5	9	3	4.5	ND	ND	ND	0.1-1.1	0.9-4
MDS/AML (yes/no)	2/6 in family[40]	2/6 in family[40]	No	Trilineage dysplasia	No	No	No	No	No	—	—
Reference	32	32	37, 38	31	UP	UP	UP	31	33, 47		

NA, Not applicable; *ND*, not determined; *UP*, unpublished.
*Range of 10 XLN patients is indicated.
†WAS L270P was reported as T843C in Devriendt et al;[32] this has changed because of updated gene browsers.
‡Values are from 3 XLN patients in the same family.[32]

I294T patients and healthy donor samples and stimulated them with CpG, CD40L, and IL-2 for 4 days; all these cells were then stimulated with IL-2, IL-10, and IL-21 for another 4 days (Fig 2, *A*). Activated naive B cells underwent robust cell proliferation (Fig 2, *B*). Naive B cells from the WAS F271S and WAS I294T patients had reduced proliferation capacity compared to healthy donor B cells, which was not caused by decreased cell viability (Fig 2, *B*). By gating at $CD27^+CD38^+CD20^{lo}$ cells, which are commonly used for analysis of PBMC plasma cells in cultured cells, too few cells could be recovered for quantification (see Fig E3, *A,* in this article's Online Repository at www.jacionline.org). However, sorted $CD27^+$ memory cells downregulated $CD27^+$ after activation while maintaining the high intracellular immunoglobulin level that is a characteristic of plasma cell differentiation (Fig E3, *B*). Instead, we first examined immunoglobulin class switching in cultured naive B cells. IgA^+ cells were comparable between control and XLN culture, whereas IgG^+ cells in XLN cultures were reduced compared to controls (Fig 2, *B,* and Fig E3, *C*). To analyze plasma cell differentiation, we gated the $CD138^+CD38^{hi}$ cells that had higher

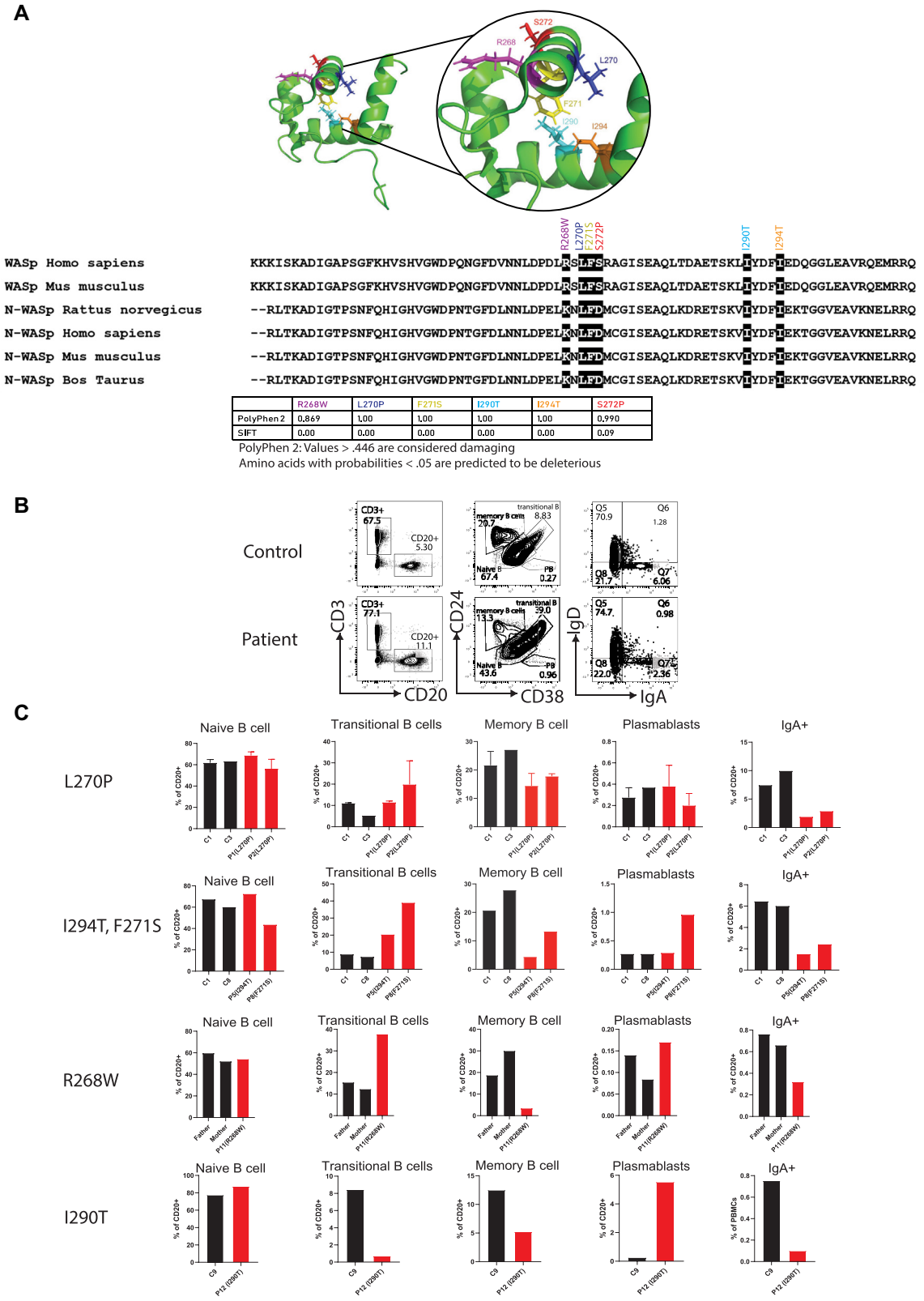

FIG 1. B-cell differentiation of peripheral blood in XLN patients. **A,** Location of amino acids identified in XLN patients in WAS protein. XLN patient mutations in WASp included R268W, L270P, F271S, I290T, I294T, and S272P. Alignment of the GBD of WASp and N-WASp is indicated across species. PolyPhen and SIFT (sorting intolerant from tolerant) prediction of XLN patient mutations is shown. **B,** Fluorescence-activated cell sorting (FACS) analysis of B-cell subsets from control and patient peripheral blood. Representative FACS plots are shown. **C,** Quantification of B-cell subsets from (*B*). *Black* indicates controls or patient family members; *red,* XLN patients. Control subjects had samples collected at the same time and location as patients' samples. Subject C1 was 37 years old; C3, 33 years; C8, 25 years; C9, 4 years; father, 50 years; and mother, 50 years.

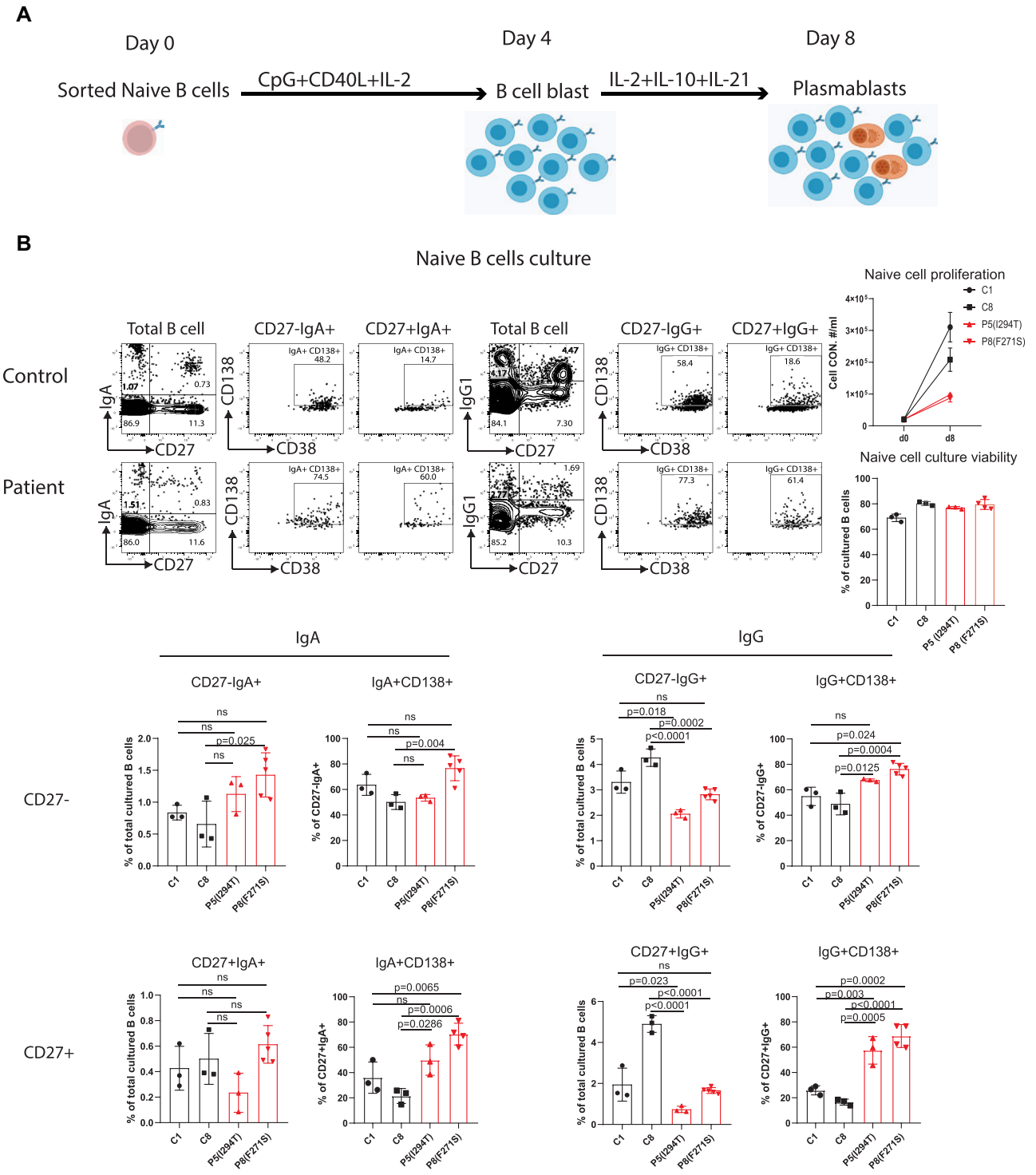

FIG 2. *In vitro* B-cell response of XLN patient naive and memory B cells. **A,** Schematics of *in vitro* culture system of human B cells. **B,** Analysis of naive B-cell culture. Shown are representative fluorescence-activated cell sorting plots and quantification of cell proliferation, cell viability, $CD27^{-}IgG^{+}$, $CD27^{-}IgA^{+}$, $CD27^{+}IgG^{+}$, $CD27^{+}IgA^{+}$, $IgG^{+}CD138^{+}$, and $IgA^{+}CD138^{+}$ cells among the switched IgA^{+} and IgG^{+} cells ($P < .0001$ controls vs patients). Data are shown as means ± SDs.

intracellular immunoglobulin level compared to the $CD138^-$ population among the switched B cells (Fig E3, *C-E*). The $CD27^-IgA^+$ and $CD27^-IgG^+$ cells were probably from the contamination of class-switched $CD27^-$ memory cells (Fig E3, *F*), and the plasma cell differentiation among these cell population was comparable between control and XLN cultures (Fig 2, *B*). The $CD27^+IgA^+$ and $CD27^+IgG^+$ represented the newly switched cells from naive B cells on activation (Fig 2, *B*). XLN B cells showed increased differentiation of IgG^+CD138^+ and IgA^+CD138^+ plasma cells among the $CD27^+IgG^+$ and $CD27^+IgA^+$ cells, respectively (Fig 2, *B,* and Fig E3, *C* and *D*). These data lead to the interesting possibility that XLN B cells generated more plasma cells at the expense of cell proliferation.

Murine XLN B cells show decreased GC B-cell response and increased plasma cell differentiation

To understand why XLN mutations were associated with increased formation of plasma cells, we analyzed B-cell development and differentiation in 2 murine XLN models that harbor WASp L272P and WASp I296T mutations, corresponding to WASp L270P and WASp I294T mutations in patients.[35,36] Wild-type (WT) and XLN mice had similar B-cell development in bone marrow (see Fig E4, *A,* in this article's Online Repository at www.jacionline.org) and normal differentiation of splenic B cells (Fig 3, *A*). WT and XLN mice had a similar proportion of $CD73^+PDL2^+CD80^+$ memory cells and total spleen $CD138^+$ plasma cells (Fig 3, *B*). GC response was examined upon SRBC immunization at day 7. XLN mice had reduced number and area of GCs (Fig 3, *C*). As measured by flow cytometry, XLN mice had a 2-fold reduction in $GL7^+CD95^+$ GC B cells compared to WT mice (Fig 3, *D*). The DZ/LZ ratio was similar between WT and XLN mice (Fig 3, *D*). In contrast, the GC response is dramatically increased in mice when WASp was conditionally deleted in B cells, with altered DZ/LZ ratio compared to WT mice.[27] Within the $CD95^+GL7^+$ GC B cells, XLN mice had increased plasma cells, defined as $CD138^+$ and $IRF4^{hi}Pax5^{lo}$ cells, compared to WT mice (Fig 3, *E*). In the competitive setting of bone marrow chimeric mice, XLN B cells showed a disadvantage in the marginal zone (MZ) B-cell lineage and similar contribution to the follicular B cells compared to WT B cells (Fig 3, *F*). $WASp^{-/-}$ B cells showed strong disadvantage in the MZ lineage cells (Fig 3, *F*).[17,25,26] XLN mice showed a 2-fold disadvantage in contribution to GC B cells (Fig 3, *G*). Surprisingly, GC $CD138^+$ plasma cells from XLN B cells were in disadvantage compared to WT GC plasma cells. This could be due to the significant lower number of XLN B cells when in competition with WT B cells in the GC; even the increased plasma cell differentiation capacity of XLN B cells was not enough to revert the disadvantage.

These data suggest that XLN B cells have higher capacity to form plasma cells in GCs, but that XLN GC B cells fail to compete with WT GC B cells in a competitive setting.

XLN mice show normal affinity maturation in response to NP-KLH

We next examined whether XLN B cells could undergo affinity maturation. Animals were immunized with NP-KLH in alum, followed by a second immunization with NP-KLH at day 21, and spleen and bone marrow B cells were examined on day 28. WT and XLN mice showed a similar generation of total spleen $CD138^+$ cells and NP^+ plasma cells (Fig 4, *A*). WASp I296T mice had reduced GC B cells compared to WT mice (Fig 4, *B*). NP^+ GC B cells and NP^+ plasma cells in GCs were comparable between WT and XLN mice (Fig 4, *B*). In the bone marrow, WT and XLN had similar proportion of total IgM^+ and IgG^+ plasma cells. IgA^+ plasma cells were reduced in WASp I296T mice and were variable in WASp L272P mice (Fig 4, *C*). NP-specific IgM and IgA plasma cells were overall low in both WT and XLN mice (Fig 4, *C*). These data, taken together, suggest that XLN mice had normal capacity to form antigen-specific plasma cells in response to NP-KLH. The differential result of XLN mice in response to SRBC and NP-KLH could reflect the difference between the primary response (SRBC) and the secondary response (NP-KLH).

To determine the antibody affinity maturation, we used ELISA to detect NP-specific antibodies of high affinity using NP8-BSA and of moderate/low affinity using NP25-BSA. WT and XLN serum samples had similar concentration of NP8- and NP25-reactive antibodies, leading to a similar NP8/NP25 ratio at day 21 and day 28 (Fig 4, *D*).

Together, these data suggest that B cells in XLN mice, despite having reduced GC B cells, undergo normal affinity maturation in response to the T-cell–dependent antigen NP-KLH.

XLN B cells have increased WASp phosphorylated tyrosine-293 and normal BCR response

To understand the molecular cause for increased plasma cell generation of XLN B cells, we examined phosphorylation of WASp tyrosine-293 (tyrosine-291 in human WASp). Phosphorylation of tyrosine-293 leads to prolonged WASp activity, even in the absence of Cdc42 binding,[41] and, together with membrane recruitment, protects WASp from degradation.[36] Compared to WT B cells, XLN B cells showed increased phospho-WASp on LPS stimulation for 24 hours (Fig 5, *A,* and Fig E4, *B*). Recruitment of phospho-WASp in proximity to the BCR is important for immune synapse formation and early BCR signaling.[24] To examine how XLN B cells rearranged the actin cytoskeleton in the BCR immune synapse, B cells were imaged using confocal microscopy on activation of the BCR through immobilized cross-linking of anti-IgM and anti-IgG antibodies. Blocking antibodies to CD19 did not induce cell spreading, whereas activating BCR engagement led to similar spreading by WT, XLN, and $WASp^{-/-}$ B cells (Fig 5, *B*). The circularity of the contact area indicated similar symmetry of WT, XLN, and $WASp^{-/-}$ B cells (Fig E4, *C*). Internalization of the BCR occurs on minutes of BCR activation. WT and XLN B cells had similar BCR surface expression, and BCR internalization occurred at a similar rate (Fig 5, *C*). WT and XLN B cells had similar upregulation of CD86 and major histocompatibility complex (MHC) class II at 60 minutes after BCR activation (Fig 5, *D* and *E*), suggesting that XLN B cells could respond to BCR activation. Taken together, XLN B cells form stable immunologic synapses after stimulation through the BCR, and BCR signaling is unaltered in XLN B cells.

Decreased immunoglobulin class switching to IgA and increased plasma cell differentiation of mouse XLN B cells occur *in vitro*

To understand B cells' intrinsic contribution to alteration in immunoglobulin class switching, we stimulated murine B cells

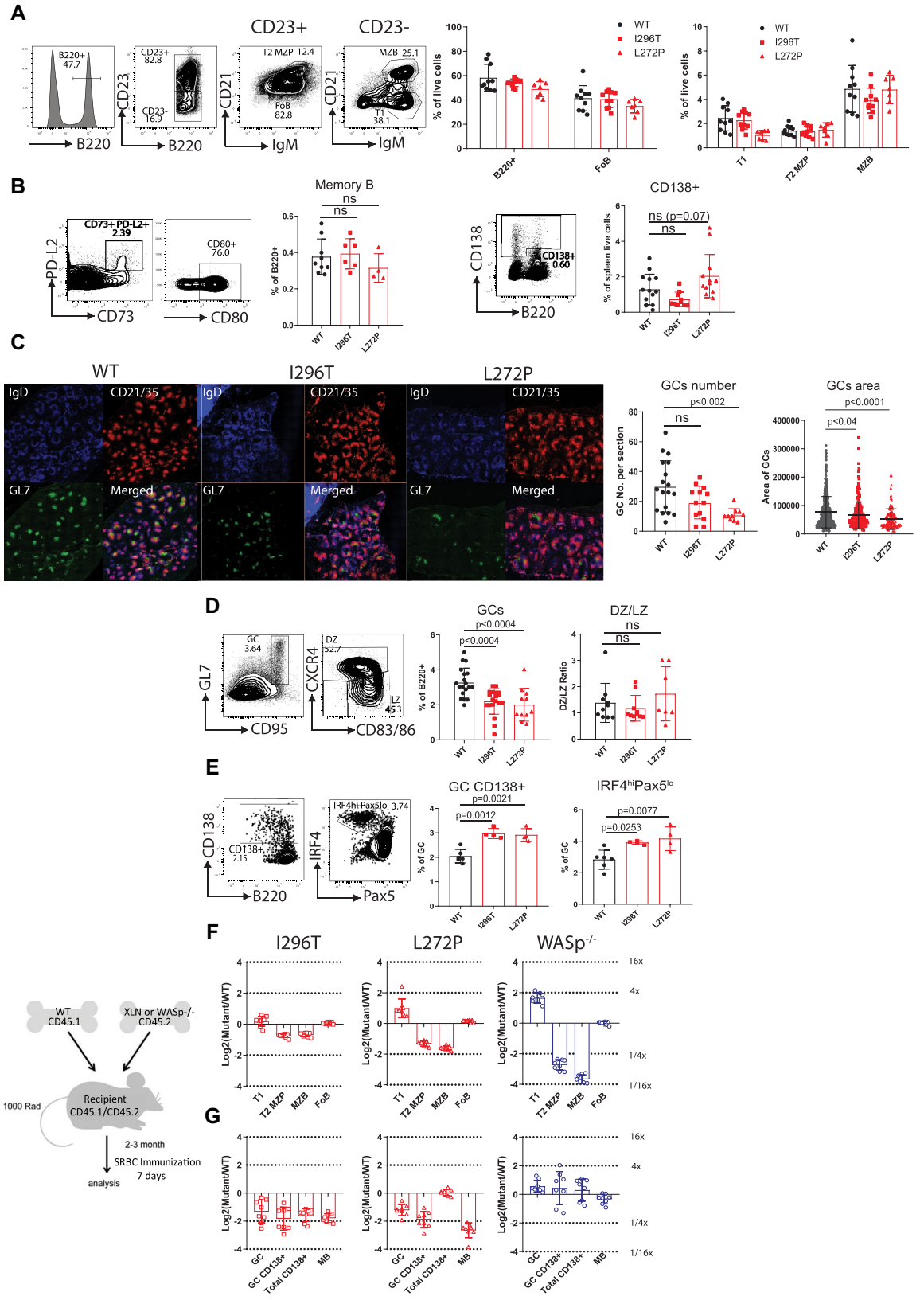

FIG 3. B-cell development and differentiation in XLN mouse models. **A,** B-cell development in mouse spleen. *Left,* Representative fluorescence-activated cell sorting (FACS) plots; *right,* quantification of total B220^{+}, follicular B cells (FoB), transitional 1 (T1), transitional 2 marginal zone progenitor (T2-MZP), and MZ B cells (n = 10, 2 experiments). **B,** Total memory B-cell and CD138^{+} plasma cell differentiation in mouse spleen. Shown are representative FACS plots and quantification (n = 4-12, 2 experiments).

in vitro to induce immunoglobulin class switching to IgG_1 (anti-CD40 antibodies + IL-4), IgG_{2b} (LPS + TGF-β), IgG_3 (LPS), and IgA (LPS + TGF-β). $WASp^{-/-}$ B cells showed increased immunoglobulin class switching to all the tested immunoglobulin isotypes compared to WT B cells (Fig 6, *A-D*). XLN B cells showed reduced immunoglobulin class switching to IgG_{2b} and IgA compared to WT cells (Fig 6, *B* and *D*). Immunoglobulin class switching to IgG_1 and IgG_3 of XLN B cells showed a milder reduction that reached significance only in one of the XLN strains (Fig 6, *A* and *C*). To examine whether compromised TGF-β signaling may explain decreased IgG_{2b} and IgA CSR, TGF-β receptor II internalization and phosphorylation of Smad 2/3 was examined. Upon TGF-β stimulation, WT and XLN B cells had similar TGF-β receptor II internalization and phosphorylation of Smad2/3 (Fig E4, *D* and *E*), suggesting intact TGF-β signaling in XLN B cells.

To further assess plasma cell generation *in vitro*, we activated naive B cells with the iGB culture system (Fig 6, *E*).[39] The earliest commitment to plasmablast/plasma cells was characterized by downregulation of Pax5 and upregulation of IRF4.[42] At day 7, XLN B cells showed a 2-fold higher proportion of $Pax5^{low}IRF4^{hi}$ plasma cells and a 2-fold increase in IgG^{hi} plasma cells compared to WT cells (Fig 6, *E*). However, addition of TGF-β to the iGB culture did not lead to CSR to IgA, which prevented us from analyzing IgA^+ plasma cell differentiation in this system. Instead, we used the cell culture system described above to activate cells with LPS + TGF-β. We found that the reduced IgA CSR of XLN B cells was associated with an increased generation of IgA^+CD138^+ plasma cells compared to WT B cells (Fig E4, *F*).

This suggests that murine XLN B cells are intrinsically defective to undergo immunoglobulin class switching, especially to IgA and IgG_{2b}, and have increased capacity to form plasma cells.

Decreased immunoglobulin class switching and increased plasma cell differentiation are due to compromised cell division of XLN B cells

Immunoglobulin CSR is directly linked to cell division.[43,44] Our data from XLN patients' B cells strongly suggest that the compromised cell proliferation could be the cause of defective class switching to IgA. To test this, we first examined the cell cycle progression of murine XLN B cells. IL-21 was added to iGB culture system at day 3 for 24 hours, and 2 rounds of cell division were measured to determine the cell cycle length and the capacity of B cells to divide (Fig 7, *A*). WT, $WASp^{-/-}$, and XLN B cells had similar cell cycle duration of about 400 minutes (see Fig E5, *A,* in this article's Online Repository at www.jacionline.org). All WT B cells showed normal cell division into 2 daughter cells (Fig 7, *A* and *B,* and see Video E1 in this article's Online Repository at www.jacionline.org). $WASp^{-/-}$ B cells showed 3.84% of B cells with defective division (Fig 7, *A* and *B,* and see Video E2 in this article's Online Repository at www.jacionline.org). XLN B cells showed 8.33% (L272P) and 13.18% (I296T) of B cells with defective cell division, such as tri-way division, and some cells that almost completed the cell division but then fused back into a single cell (Fig 7, *A* and *B,* and see Videos E3 and E4 in this article's Online Repository at www.jacionline.org). We reasoned that the abnormal cell division could limit the capacity of XLN B cells to reach a high division number, which in turn compromised the CSR to IgA, which requires 7 or 8 cell divisions (Fig E5, *B* and *C*). Indeed, cell-tracing violet tracking of cell divisions of *in vitro* B-cell culture showed a reduction of XLN B cells that reached division 8 compared to WT and $WASp^{-/-}$ B cells (Fig 7, *C*). In addition, I296T cells at division 8 showed reduced CSR to IgA, and L272P had comparable level of IgA compared to WT cells, while $WASp^{-/-}$ cells showed increased CSR to IgA. Although class switching to IgG_{2b} was already apparent after 4 or 5 division (Fig E5, *C*), XLN B cells showed compromised CSR to IgG_{2b} within each division compared to WT cells, which was in contrast to $WASp^{-/-}$ cells that showed increased CSR to IgG_{2b} (Fig 7, *C*). This suggests that the CSR defect of XLN B cells was not limited to IgA, and relatively milder defects of other isotypes compared to IgA could be due to their earlier appearance and accumulation of switched cells during successive divisions (Fig E5, *B-D*).

Previous work from cell lines shows that the XLN mutation WAS I294T can induce aberrant cytokinesis caused by elevated F-actin that leads to increased genomic instability.[45] Activation-induced cytidine deaminase induced ectopic genotoxic stress has been suggested to promote plasma cell differentiation by upregulation of Blimp1.[46] It is plausible that defective cell division was associated with increased plasma cell generation in XLN B cells, possibly caused by increased genomic instability, as previously shown for XLN B cells.[35] To test this reasoning, we examined plasma cell differentiation of activated B cells that underwent activation-induced cytidine deaminase–induced genotoxic stress in WT and WASp I296T mice. DNA double-strand breaks were detected by phosphorylation of γH2AX and/or γH2AX. Among the activated B cells with genotoxic stress ($CD95^+\gamma H2AX^+$), there was a significant increase of the $IRF4^{hi}Pax5^{lo}$ plasma cells compared to total activated $CD95^+$ B cells (Fig E5, *E* and *F*). Moreover, WASp I296T GC B cells indeed showed significant increase of genomic instability as marked by γH2AX, and increased $IRF4^{hi}Pax5^{lo}$ cell population compared to WT GC B cells (Fig 7, *D*).

These data suggest that XLN B cells have reduced IgA CSR and favor the plasma cell fate as a result of the increased genotoxic stress resulting from aberrant cell division during activation and clonal expansion.

C, Immunohistochemistry of spleen sections immunized with SRBC for 7 days. *Left,* Representative microscopy images; *right,* quantification of GC number and area. **D,** GC response upon SRBC immunization for 7 days. *Left,* Representative FACS plots; *right,* quantification of GC B cells (n = 11-18, 3 experiments) and DZ/LZ ratio (n = 7-10, 2 experiments). **E,** Plasma cell differentiation from the GC response. *Left,* Representative FACS plots of $CD138^+$ and $IRF4^{hi}Pax5^{lo}$ cells among GC B cells; *right,* quantification (3-5 mice per group, 1 representative experiment from 3 performed). **F,** B-cell development in spleen of bone marrow chimeric mice; *y-axis,* log_2 of measured XLN/WT to grafted XLN/WT ratio, or measured $WASp^{-/-}$/WT to grafted $WASp^{-/-}$/WT ratio. **G,** GC response in bone marrow chimeric mice; *y-axis,* log_2 of measured XLN/WT to grafted XLN/WT ratio, or measured $WASp^{-/-}$/WT to grafted $WASp^{-/-}$/WT ratio (n = 8, 2 experiments). One-way ANOVA. Data are shown as means ± SDs.

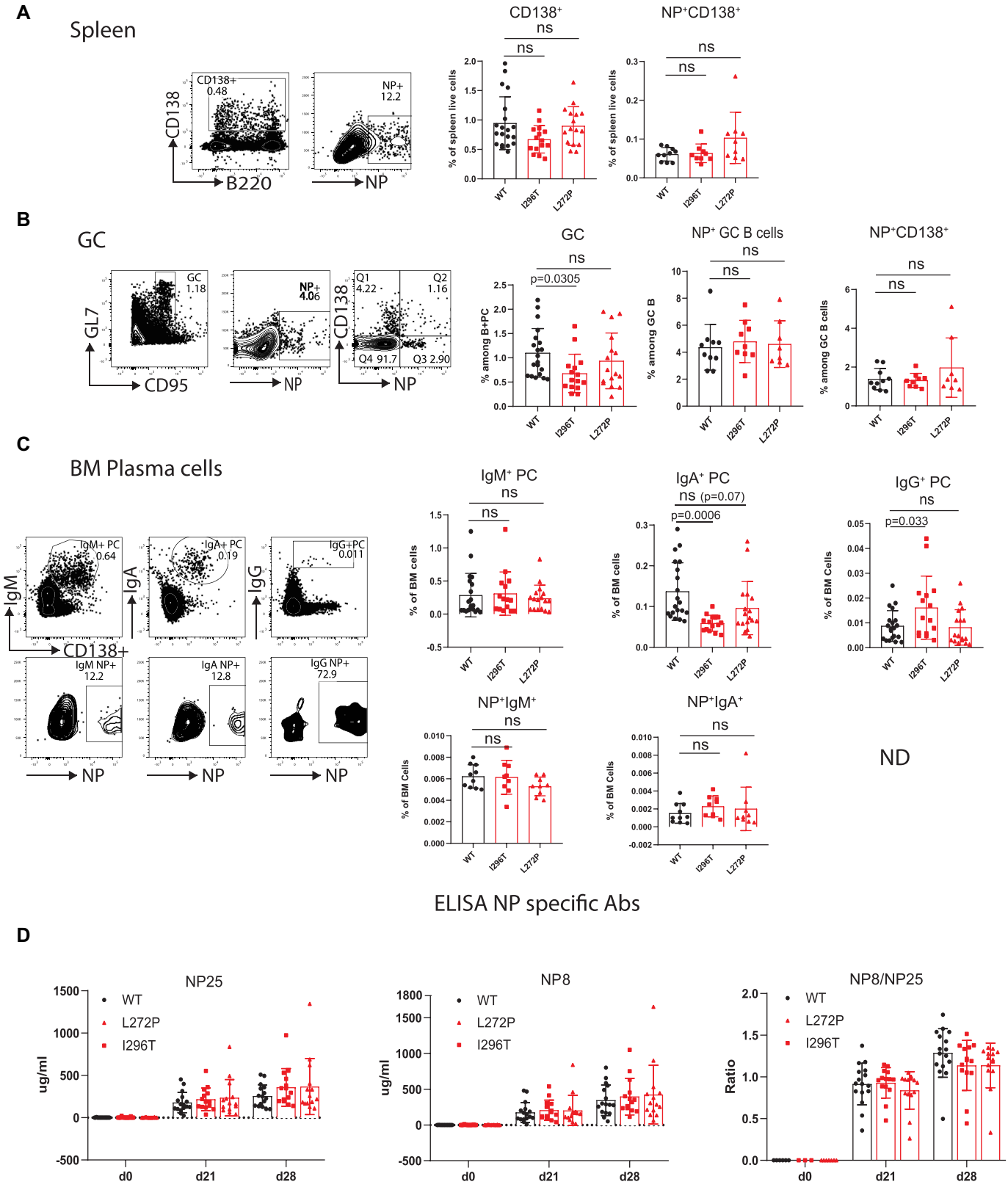

FIG 4. Antigen-specific B-cell response to NP-KLH in XLN mouse models. **A,** Total plasma cells ($CD138^+$) and NP-specific plasma cells (NP^+CD138^+) in spleen on NP-KLH immunization at day 28. *Left,* Representative fluorescence-activated cell sorting (FACS) plots; *right,* quantification (n = 15-20, 2 experiments). **B,** GC response on NP-KLH immunization at day 28. *Left,* Representative FACS plots; *right,* quantification of GC B cells, NP-specific GC B cells (NP^+ GC B), and NP-specific plasma cells derived from GC (NP^+CD138^+) (n = 15-20, 2 experiments). **C,** Plasma cells and NP-specific plasma cells in bone marrow. *Left,* Representative FACS plots; *right,* quantification of IgM^+, IgA^+, and IgG^+ plasma cells and NP-specific IgM^+ and IgA^+ plasma cells (n = 15-20, 2 experiments). **D,** NP-specific antibody response. Serum levels of low/intermediate affinity antibody (NP25) and high-affinity antibody (NP8) against NP. Antibody affinity maturation over time measured by NP8/NP25 ratio (n = 14-15, 2 experiments). One-way ANOVA. Data are shown as means ± SDs.

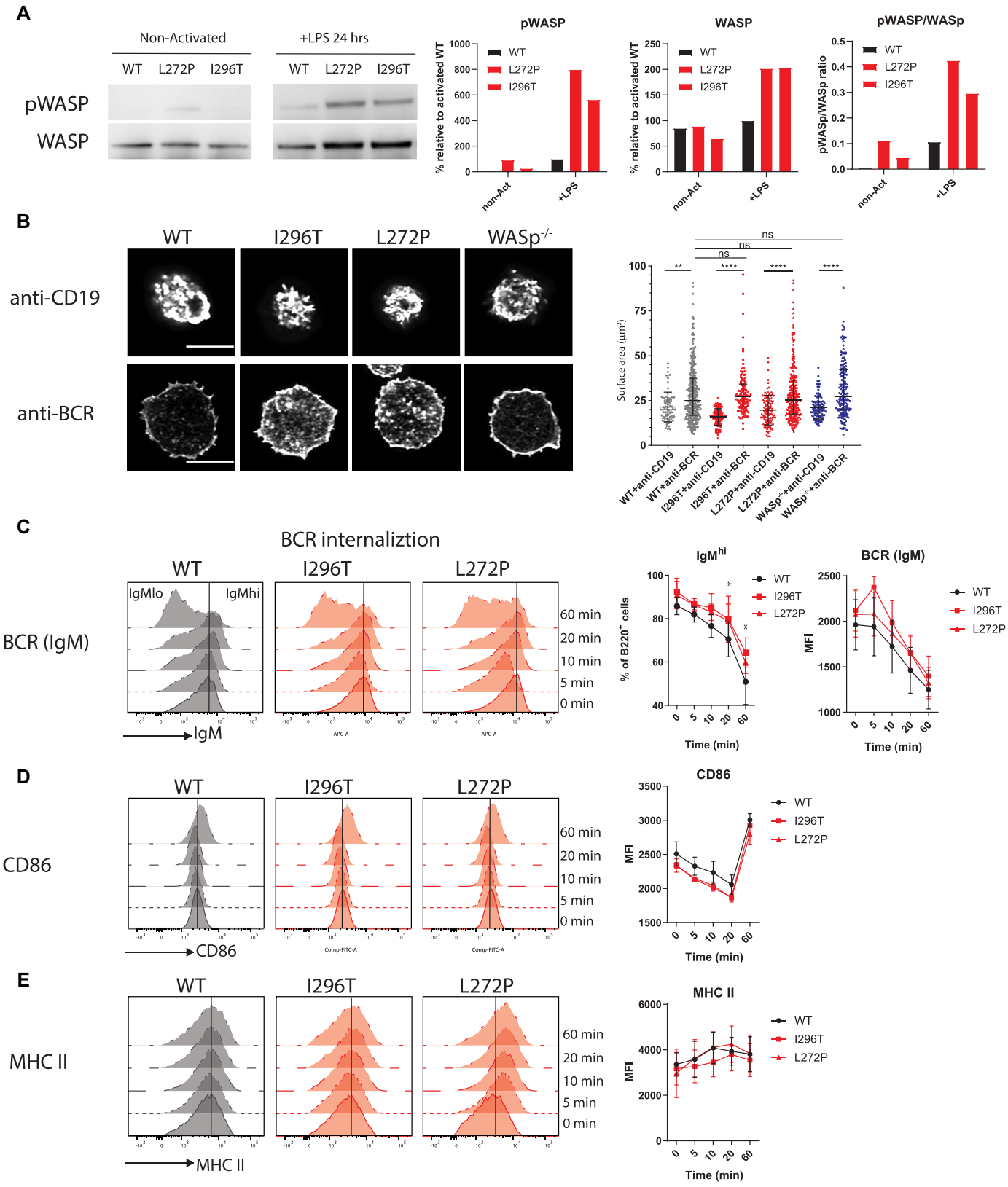

FIG 5. Activation status of XLN B cells stimulated *in vitro*. **A,** Phosphorylation of WASp on LPS stimulation. Western blot test was performed to detect WASp phosphorylation (*left*) and quantification (*right*). **B,** B-cell spreading on CD19 and BCR activation. Shown are representative images and quantification of spreading area. **C,** BCR internalization on anti-IgM stimulation. *Left,* Histogram overlay at indicated time points; *right,* quantification of percentage of IgM^{hi} cells or surface IgM MFI. **D,** Level of B-cell activation marker CD86 on anti-IgM stimulation. *Left,* Histogram overlay at indicated time points; *right,* quantification of surface CD86 MFI. **E,** MHC II level on anti-IgM stimulation. *Left,* Histogram overlay at indicated time points; *right,* quantification of surface MHC II MFI (experiments repeated 3 times). Data are shown as means ± SDs.

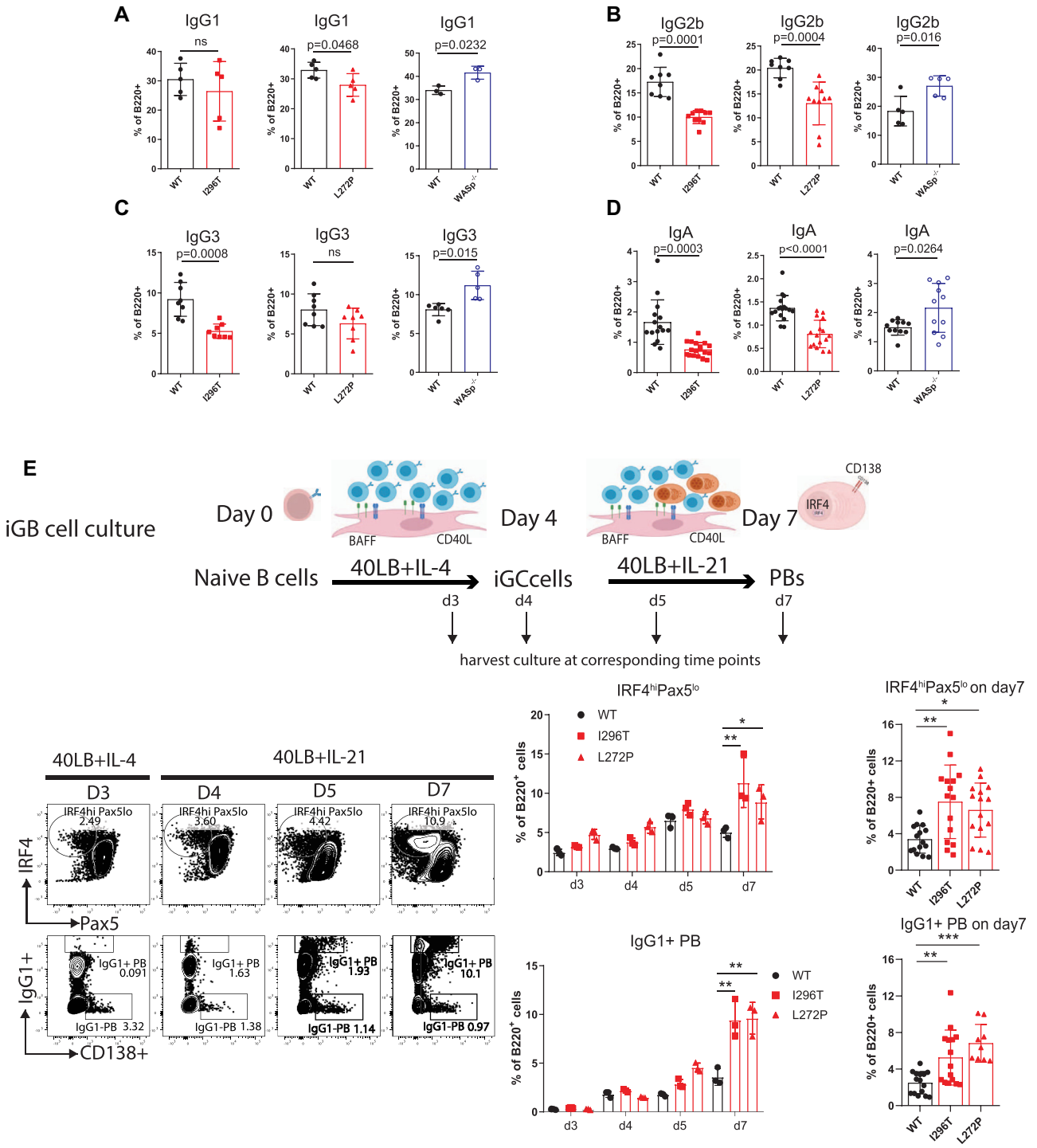

FIG 6. Immunoglobulin class switching and plasma cell differentiation in XLN mouse B cells. Immunoglobulin class switching to IgG_1 (**A**), IgG_{2b} (**B**), IgG_3 (**C**), and IgA (**D**) of the *in vitro* activated mouse B cells (*in vitro* experiment repeated 3 to 17 times depending on immunoglobulin isotype). Unpaired *t* test. **E,** Plasma cell differentiation of inducible GC B cells. Schematics of inducible GC B-cell culture system (iGB culture). Representative fluorescence-activated cell sorting plots of $IRF4^{hi}Pax5^{lo}$ cells and IgG^+ cells (*left*) kinetic changes from day 3 to day 7 in 1 representative experiment, and (*right*) quantification of pooled data on day 7 from 6 experiments. Two-way ANOVA. $*P < .05$, $**P < .01$, $***P < .001$.

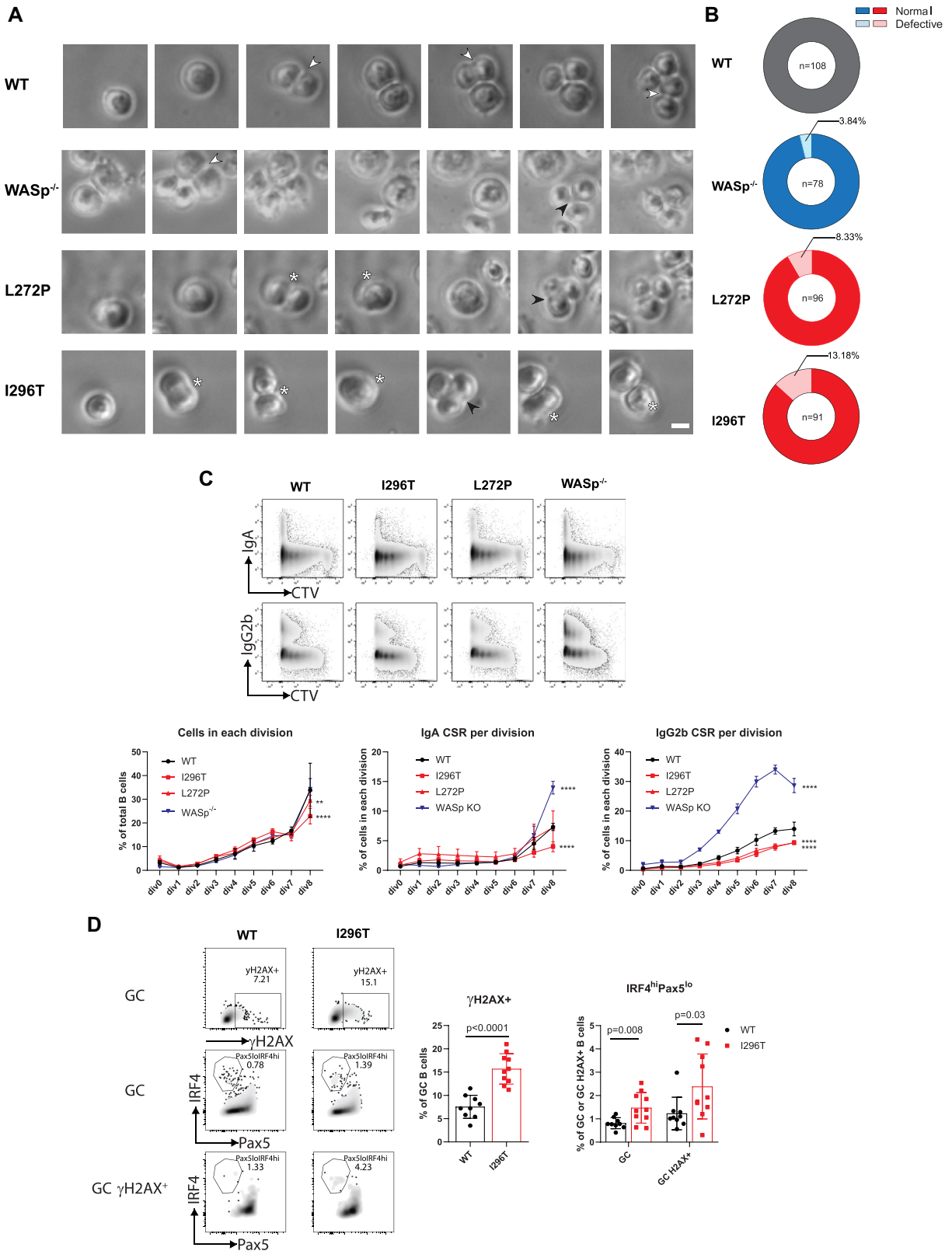

FIG 7. XLN B-cell division, immunoglobulin class switching, and plasma cell differentiation. **A,** B-cell division of iGB cells measured by time-lapse microscopy at 24 hours on addition of IL-21 at day 4. *White arrow* indicates normal division into 2 daughter cells; *black arrow,* 3-way division; and *white star,* failure to divide into 2 daughter cells. **B,** Quantification of cells with normal and abnormal divisions. **C,** Class switching to IgA and IgG_{2b} in relation to cell divisions. Representative fluorescence-activated cell sorting (FACS) plots and quantification of proliferating cells in each division, and IgA or IgG_{2b} CSR in each division. Statistical analysis performed for cells at division 8 by 2-way ANOVA (n = 6, 2 experiments). **D,** Genotoxic stress and plasma cell differentiation of GC B cells. Shown are representative FACS plots and quantification of $\gamma H2AX^+$ among GC B cells, and $IRF4^{hi}Pax5^{lo}$ cells among GC and GC $gH2AX^+$ B cells. Unpaired *t* test or 2-way ANOVA (n = 9-10, 2 experiments).

DISCUSSION

Coordinated regulation of actin dynamics is a prerequisite for normal B-cell responses, as is increasingly evident from the expanding recognition of primary immunodeficiency diseases with mutations in actin regulators.[15,47] Here, we studied overactive WASp in XLN patients and animal models and found that increased WASp activity leads to aberrant GC responses and premature generation of plasma cells. Our data from studying B cells with overactive WASp suggest that GC B cells with increased genomic instability may slow down proliferation and upregulate IRF4 and thereby differentiate into plasma cells faster, perhaps as a way to avoid B-cell transformation into lymphoma. The compromised cell proliferation and faster plasma cell output from GC would explain both the reduced GC response in XLN mice and the defective immunoglobulin class switching *in vitro* of XLN B cells. Together with the compromised cell proliferation of naive B cells *in vitro* from XLN patients, it is likely that low numbers of IgA^+ B cells in XLN patients is caused by failure to undergo enough rounds of cell division, as is especially apparent for CSR to IgA, which requires 7 or 8 cell divisions. The relative milder defect of CSR to the IgG isotypes is likely a result of an early appearance and accumulation of switched B cells during successive divisions.

XLN patients have congenital neutropenia in childhood leading to recurrent severe bacterial infections. Despite the low neutrophil number in blood, the number of neutrophils in their saliva is normal (Table I),[36] suggesting that neutrophils accumulate in tissues. Importantly, this notion is supported by the relatively mild clinical symptoms of XLN patients compared to other types of severe congenital neutropenia, especially with increased age.[31-33,36] Low serum IgA has been described in several XLN patients from a large WAS I294T kindred.[33,48] We show in this study that low CSR to IgA is a characteristic of XLN patient and murine B cells. This leads us to propose 4 characteristic features of XLN patients: severe congenital neutropenia, mutations in the WAS-GBD predicted to be disruptive, low IgA^+ B cells, and neutrophils present in saliva.

Importantly, previous work by us and others, together with our findings here, suggest a critical role of WASp in maintaining an efficient GC response. Conditional deletion of WASp in B cells leads to increased GC response, and lack of both WASp and N-WASp results in reduced GC and compromised somatic hypermutation. Moreover, complete knockout of WASp in mouse models leads to reduced GC response, which is probably due to greatly compromised T-cell function.[20,21,25,26] A puzzling finding of the XLN mice studied here is that despite forming smaller GC and having higher plasma cell output in response to SRBC, XLN B cells had normal affinity maturation in response to NP-KLH immunization and produced normal titers of high-affinity NP-specific antibodies. Although there is increased phosphorylation at tyrosine-293 of XLN-WASp that can mediate increased cytoplasmic F-actin and migration (this study),[16,36] chemotaxis of murine B cells toward CXCL12 is normal.[35] Therefore, it is possible that the XLN mutations in WASp have little impact on interzonal migration of GC B cells, leading to a normal DZ/LZ ratio. This is in contrast to mice lacking WASp or WASp and N-WASp in B cells, with altered GC architecture and LZ/DZ ratio.[20,21,25,26] WT and XLN B cells showed similar B-cell spreading on anti-IgM/IgG activation and had normal BCR internalization, indicating an unperturbed assembly of the immune synapse of XLN B cells when capturing antigen and normal affinity discrimination mediated by dynamic actin and myosin contraction. Therefore, the small GC may solely result from reduced cell proliferation and increased plasma cell output in XLN mice. These data suggest that increased plasma cell output can compensate for decreased GC response, so total and NP-specific plasma cell generation in response to NP-KLH was comparable between XLN and WT mice. Plasma cells can be generated from both the GC response and the extrafollicular pathway. It is possible that XLN B-cell activation in the extrafollicular pathway is unperturbed, but it contributes a significant amount of plasma cells to the total plasma cell pool. Moreover, the limited niche to support plasma cell survival may restrain the total number of plasma cells in the organism.[49]

Immunoglobulin CSR is directly coupled to cell division, and the failure of XLN B cells to undergo normal cell division explains the decreased CSR to IgA. Importantly, a single cell division error leading to chromosomal bridge formation by actomyosin forces can induce missegregated chromosomes, which may rapidly evolve to generate additional mutations and chromosomal aberrations after cell division.[50] Surprisingly, rather than increased cell death, as might be expected from failure to divide, this was associated with increased generation of plasma cells by XLN B cells and indicates a B-cell–intrinsic pathway to differentiate DNA-damaged cells into plasma cells. In support of this reasoning, we found an increased proportion of plasma cells within the cell population that harbors DNA double-strand breaks labeled with phospho-γH2AX compared to total activated $CD95^+$ B cells. GC B cells with high DNA damage load would differentiate into the terminally differentiated and quiescent plasma cell subset, which could act as an additional safeguard against B-cell transformation. In support of this reasoning, we did not detect increased lymphoma development when breeding the XLN mice onto a p53 heterozygous background,[51] and lymphoma has not been described in XLN patients. We conclude that the GC reaction *per se* could prevent development of B-cell transformation by accelerating the plasma cell output at the expense of B-cell proliferation and CSR.

In contrast to B-cell dysfunction caused by WASp deficiency that is characterized by reduced marginal zone B cells, spontaneous GC formation, and production of autoantibodies, our data suggest that WAS XLN mutations lead to a relatively milder defect in the cells response. The increased abnormal cell division compromised cell proliferation of XLN B cells, which leads to increased genotoxic stress, defective immunoglobulin switching, reduced GC response, and premature plasma cell formation. Although the specific antibody response and affinity maturation remain intact in the XLN mouse models, clinical data of vaccine responses of XLN patients suggest reduced response to childhood vaccinations (see Table E1 in this article's Online Repository at www.jacionline.org). This, together with defective production of IgA, the main antibody isotype lining the mucosa system, provides an additional explanation in addition to neutropenia for the recurrent bacterial infections that occur in XLN patients.

We are grateful to the XLN patients and their families for supporting our study. We thank the staff of the Department of Microbiology Tumor and Cell Biology and KMA animal facility and the Biomedicum Imaging Core Facility.

Key messages

- **XLN patients with overactive WASp have decreased memory B cells, reduced IgA$^+$ cells, and impaired cell proliferation.**
- **Overactive mutations in WASp lead to abnormal B-cell division and premature generation of plasma cells *in vitro* and *in vivo*.**

REFERENCES

1. Muramatsu M, Kinoshita K, Fagarasan S, Yamada S, Shinkai Y, Honjo T. Class switch recombination and hypermutation require activation-induced cytidine deaminase (AID), a potential RNA editing enzyme. Cell 2000;102:553-63.
2. Liu D, Xu H, Shih C, Wan Z, Ma X, Ma W, et al. T-B-cell entanglement and ICOSL-driven feed-forward regulation of germinal centre reaction. Nature 2015; 517(7533):214-8.
3. Shulman Z, Gitlin AD, Weinstein JS, Lainez B, Esplugues E, Flavell RA, et al. Dynamic signaling by T follicular helper cells during germinal center B cell selection. Science 2014;345(6200):1058-62.
4. Gitlin AD, Shulman Z, Nussenzweig MC. Clonal selection in the germinal centre by regulated proliferation and hypermutation. Nature 2014;509(7502):637-40.
5. Victora GD, Schwickert TA, Fooksman DR, Kamphorst AO, Meyer-Hermann M, Dustin ML, et al. Germinal center dynamics revealed by multiphoton microscopy with a photoactivatable fluorescent reporter. Cell 2010;143:592-605.
6. Krautler NJ, Suan D, Butt D, Bourne K, Hermes JR, Chan TD, et al. Differentiation of germinal center B cells into plasma cells is initiated by high-affinity antigen and completed by Tfh cells. J Exp Med 2017;214:1259-67.
7. Natkanski E, Lee WY, Mistry B, Casal A, Molloy JE, Tolar P. B cells use mechanical energy to discriminate antigen affinities. Science 2013;340(6140):1587-90.
8. Tolar P, Spillane KM. Force generation in B-cell synapses: mechanisms coupling B-cell receptor binding to antigen internalization and affinity discrimination. Adv Immunol 2014;123:69-100.
9. De Silva NS, Klein U. Dynamics of B cells in germinal centres. Nat Rev Immunol 2015;15:137-48.
10. Li X, Gadzinsky A, Gong L, Tong H, Calderon V, Li Y, et al. Cbl ubiquitin ligases control B cell exit from the germinal-center reaction. Immunity 2018;48:530-41.e6.
11. Scharer CD, Barwick BG, Guo M, Bally APR, Boss JM. Plasma cell differentiation is controlled by multiple cell division-coupled epigenetic programs. Nat Commun 2018;9:1698.
12. Weisel FJ, Zuccarino-Catania GV, Chikina M, Shlomchik MJ. A temporal switch in the germinal center determines differential output of memory B and plasma cells. Immunity 2016;44:116-30.
13. Moulding DA, Record J, Malinova D, Thrasher AJ. Actin cytoskeletal defects in immunodeficiency. Immunol Rev 2013;256:282-99.
14. Massaad MJ, Ramesh N, Geha RS. Wiskott-Aldrich syndrome: a comprehensive review. Ann N Y Acad Sci 2013;1285:26-43.
15. He M, Westerberg LS. Congenital defects in actin dynamics of germinal center B cells. Front Immunol 2019;10:296.
16. Westerberg L, Larsson M, Hardy SJ, Fernandez C, Thrasher AJ, Severinson E. Wiskott-Aldrich syndrome protein deficiency leads to reduced B-cell adhesion, migration, and homing, and a delayed humoral immune response. Blood 2005;105:1144-52.
17. Westerberg LS, de la Fuente MA, Wermeling F, Ochs HD, Karlsson MC, Snapper SB, et al. WASP confers selective advantage for specific hematopoietic cell populations and serves a unique role in marginal zone B-cell homeostasis and function. Blood 2008;112:4139-47.
18. Meyer-Bahlburg A, Becker-Herman S, Humblet-Baron S, Khim S, Weber M, Bouma G, et al. Wiskott-Aldrich syndrome protein deficiency in B cells results in impaired peripheral homeostasis. Blood 2008;112:4158-69.
19. Becker-Herman S, Meyer-Bahlburg A, Schwartz MA, Jackson SW, Hudkins KL, Liu C, et al. WASp-deficient B cells play a critical, cell-intrinsic role in triggering autoimmunity. J Exp Med 2011;208:2033-42.
20. Dahlberg CI, Torres ML, Petersen SH, Baptista MA, Keszei M, Volpi S, et al. Deletion of WASp and N-WASp in B cells cripples the germinal center response and results in production of IgM autoantibodies. J Autoimmun 2015;62:81-92.
21. Volpi S, Santori E, Abernethy K, Mizui M, Dahlberg CI, Recher M, et al. N-WASP is required for B-cell–mediated autoimmunity in Wiskott-Aldrich syndrome. Blood 2016;127:216-20.
22. Kolhatkar NS, Brahmandam A, Thouvenel CD, Becker-Herman S, Jacobs HM, Schwartz MA, et al. Altered BCR and TLR signals promote enhanced positive selection of autoreactive transitional B cells in Wiskott-Aldrich syndrome. J Exp Med 2015;212:1663-77.
23. Castiello MC, Bosticardo M, Pala F, Catucci M, Chamberlain N, van Zelm MC, et al. Wiskott-Aldrich syndrome protein deficiency perturbs the homeostasis of B-cell compartment in humans. J Autoimmun 2014;50:42-50.
24. Liu C, Bai X, Wu J, Sharma S, Upadhyaya A, Dahlberg CI, et al. N-wasp is essential for the negative regulation of B cell receptor signaling. PLoS Biol 2013;11: e1001704.
25. Recher M, Burns SO, de la Fuente MA, Volpi S, Dahlberg C, Walter JE, et al. B cell–intrinsic deficiency of the Wiskott-Aldrich syndrome protein (WASp) causes severe abnormalities of the peripheral B-cell compartment in mice. Blood 2012; 119:2819-28.
26. Westerberg LS, Dahlberg C, Baptista M, Moran CJ, Detre C, Keszei M, et al. Wiskott-Aldrich syndrome protein (WASP) and N-WASP are critical for peripheral B-cell development and function. Blood 2012;119:3966-74.
27. Pala F, Morbach H, Castiello MC, Schickel JN, Scaramuzza S, Chamberlain N, et al. Lentiviral-mediated gene therapy restores B cell tolerance in Wiskott-Aldrich syndrome patients. J Clin Invest 2015;125:3941-51.
28. Castiello MC, Scaramuzza S, Pala F, Ferrua F, Uva P, Brigida I, et al. B-cell reconstitution after lentiviral vector-mediated gene therapy in patients with Wiskott-Aldrich syndrome. J Allergy Clin Immunol 2015;136:692-702.e2.
29. Campellone KG, Welch MD. A nucleator arms race: cellular control of actin assembly. Nat Rev Mol Cell Biol 2010;11:237-51.
30. Kim AS, Kakalis LT, Abdul-Manan N, Liu GA, Rosen MK. Autoinhibition and activation mechanisms of the Wiskott-Aldrich syndrome protein. Nature 2000; 404(6774):151-8.
31. Ancliff PJ, Blundell MP, Cory GO, Calle Y, Worth A, Kempski H, et al. Two novel activating mutations in the Wiskott-Aldrich syndrome protein result in congenital neutropenia. Blood 2006;108:2182-9.
32. Devriendt K, Kim AS, Mathijs G, Frints SG, Schwartz M, Van Den Oord JJ, et al. Constitutively activating mutation in WASP causes X-linked severe congenital neutropenia. Nat Genet 2001;27:313-7.
33. Beel K, Cotter MM, Blatny J, Bond J, Lucas G, Green F, et al. A large kindred with X-linked neutropenia with an I294T mutation of the Wiskott-Aldrich syndrome gene. Br J Haematol 2009;144:120-6.
34. Derry JM, Ochs HD, Francke U. Isolation of a novel gene mutated in Wiskott-Aldrich syndrome. Cell 1994;79, following 922.
35. Westerberg LS, Meelu P, Baptista M, Eston MA, Adamovich DA, Cotta-de-Almeida V, et al. Activating WASP mutations associated with X-linked neutropenia result in enhanced actin polymerization, altered cytoskeletal responses, and genomic instability in lymphocytes. J Exp Med 2010;207:1145-52.
36. Keszei M, Record J, Kritikou JS, Wurzer H, Geyer C, Thiemann M, et al. Constitutive activation of WASp in X-linked neutropenia renders neutrophils hyperactive. J Clin Invest 2018.
37. Arwani M, Lee D, Haddad A, Mewawalla P. A novel mutation in Wiskott-Aldrich gene manifesting as macrothrombocytopenia and neutropenia. BMJ Case Rep 2018;2018.
38. Xia Y, Huang Y, Huang YY, Yang J. [X-linked neutropenia caused by gain-of-function mutation in *WAS* gene: two cases report and literature review]. Zhonghua Er Ke Za Zhi 2019;57:631-5.
39. Nojima T, Haniuda K, Moutai T, Matsudaira M, Mizokawa S, Shiratori I, et al. *In-vitro* derived germinal centre B cells differentially generate memory B or plasma cells *in vivo*. Nat Commun 2011;2:465.
40. Beel K, Vandenberghe P. G-CSF receptor (CSF3R) mutations in X-linked neutropenia evolving to acute myeloid leukemia or myelodysplasia. Haematologica 2009; 94:1449-52.
41. Torres E, Rosen MK. Contingent phosphorylation/dephosphorylation provides a mechanism of molecular memory in WASP. Mol Cell 2003;11:1215-27.
42. Nutt SL, Hodgkin PD, Tarlinton DM, Corcoran LM. The generation of antibody-secreting plasma cells. Nat Rev Immunol 2015;15:160-71.
43. Deenick EK, Hasbold J, Hodgkin PD. Switching to IgG3, IgG2b, and IgA is division linked and independent, revealing a stochastic framework for describing differentiation. J Immunol 1999;163:4707-14.
44. Hodgkin PD, Lee JH, Lyons AB. B cell differentiation and isotype switching is related to division cycle number. J Exp Med 1996;184:277-81.
45. Moulding DA, Blundell MP, Spiller DG, White MR, Cory GO, Calle Y, et al. Unregulated actin polymerization by WASp causes defects of mitosis and cytokinesis in X-linked neutropenia. J Exp Med 2007;204:2213-24.
46. Sherman MH, Kuraishy AI, Deshpande C, Hong JS, Cacalano NA, Gatti RA, et al. AID-induced genotoxic stress promotes B cell differentiation in the germinal center via ATM and LKB1 signaling. Mol Cell 2010;39:873-85.
47. Saeed MB, Record J, Westerberg LS. Two sides of the coin: cytoskeletal regulation of immune synapses in cancer and primary immune deficiencies. Int Rev Cell Mol Biol 2020;356:1-97.

48. Cryan EF, Deasy PF, Buckley RJ, Greally JF. Congenital neutropenia and low serum immunoglobulin A: description and investigation of a large kindred. Thymus 1988;11:185-99.
49. Wilmore JR, Allman D. Here, there, and anywhere? Arguments for and against the physical plasma cell survival niche. J Immunol 2017;199: 839-45.
50. Umbreit NT, Zhang CZ, Lynch LD, Blaine LJ, Cheng AM, Tourdot R, et al. Mechanisms generating cancer genome complexity from a single cell division error. Science 2020;368(6488):eaba0712.
51. Keszei M, Kritikou JS, Sandfort D, He M, Oliveira MMS, Wurzer H, et al. Wiskott-Aldrich syndrome gene mutations modulate cancer susceptibility in the $p53^{+/-}$ murine model. Oncoimmunology 2018;7:e1468954.